JOURNAL OF Materials CHEMISTRY

In situ Raman spectroscopic studies of $LiNi_xMn_{2-x}O_4$ thin film cathode materials for lithium ion secondary batteries

Kaoru Dokko, Mohamed Mohamedi,* Naomi Anzue, Takashi Itoh and Isamu Uchida

Department of Applied Chemistry, Faculty of Engineering, Tohoku University, Aramaki Aoba 07, Aoba-ku, Sendai 980-8579, Japan.
E-mail: mohamed@est.che.tohoku.ac.jp

Received 11th July 2002, Accepted 10th September 2002
First published as an Advance Article on the web 27th September 2002

Chemical states and structural changes accompanying the electrochemical Li extraction and insertion of $LiNi_xMn_{2-x}O_4$ ($0 < x < 0.5$) thin films in $LiBF_4$–EC–DMC solutions, studied by *in situ* Raman spectroscopy, are reported for the first time. *Ex situ* Raman measurements for the virgin electrodes revealed that the oxidation state of Ni in the pristine thin films was Ni^{2+}. *In situ* Raman spectra of the thin films collected in the organic electrolyte during Li ion extraction and insertion in the potential range 3.4–5.0 V *vs.* Li/Li^+ showed a new Raman band at 540 cm^{-1} appearing around 4.7 V, which is attributed to the Ni^{4+}–O bond. In addition, from the *in situ* Raman spectral changes, it is suggested that Li ion extraction and insertion proceed as follows: the redox of $Ni^{2+/3+}$ takes place in the potential range 4.4–4.7 V, and $Ni^{3+/4+}$ in the 4.7–5.0 V range, while the redox at 3.8–4.4 V corresponds to $Mn^{3+/4+}$. Furthermore, it was confirmed that these changes in the Raman spectra were reversible upon changing the electrode potential, and the Li ion extraction and insertion proceed in a reversible manner.

Introduction

Lithium ions can be electrochemically extracted from/inserted into spinel-related lithium manganese oxide, $LiMn_2O_4$, at 4 V *vs.* Li/Li^+.[1–4] In the spinel structure, manganese ions are in the octahedral 16d sites and lithium ions are in the tetragonal 8a sites.[3] It is relatively easy to synthesize the manganese-substituted spinel $LiM_xMn_{2-x}O_4$ (M = Li, Cr, Ni, Co, *etc.*) and numerous investigations, such as crystallographic and electrochemical studies, of such materials have been reported.[5–13] These materials are now attractive candidates as cathodes for lithium ion batteries because they can increase the cell voltage to 5 V from the present 4 V. Among this series of materials, Sigala and co-workers[14] were the first to report the charge–discharge ability of $LiCr_xMn_{2-x}O_4$ at 5 V *vs.* Li/Li^+. Similar electrochemical properties around 5 V have been reported for the spinel $LiM_xMn_{2-x}O_4$ (M = Ni, Co, Fe, Cu).[15–19] $LiNi_xMn_{2-x}O_4$ shows good stability on repeated Li ion extraction and insertion, making it the most attractive material for practical use.[15,20–22] According to the charge–discharge measurements reported by Zhong *et al.*,[15] lithium extraction from $LiNi_xMn_{2-x}O_4$ occurs at 4.7 V, where Ni^{2+} is oxidized to Ni^{4+}. This reaction was recently documented from X-ray diffraction (XRD)[23] and by X-ray absorption fine structure (XAFS) measurements.[24]

In this paper: (i) we report on the synthesis of $LiNi_xMn_{2-x}O_4$ thin films using the electrostatic spray deposition (ESD) method. Thin films thus prepared were characterized using X-ray diffraction and Raman spectroscopy. (ii) We then present *in situ* Raman spectra recorded during lithium extraction from/insertion into $LiNi_xMn_{2-x}O_4$ in the potential range 3.5–5.0 V. The dependence of Raman spectral change on electrode potential is discussed in connection with Li ion concentration and the oxidation states of manganese and nickel in the structure. This will help to clarify the valence state in $LiNi_xMn_{2-x}O_4$ and characterize the electronic and structural changes that occur upon lithiation/delithiation.

Experimental

Preparation of thin film $LiNi_xMn_{2-x}O_4$ electrodes

Thin films of $LiNi_xMn_{2-x}O_4$ were prepared by the electrostatic spray deposition (ESD) technique. Deposition conditions were similar to those reported previously.[25] Briefly, a dc voltage of 12 kV was applied between a metal capillary nozzle (inner diameter: 0.8 mm) and an electrically conductive substrate, consisting of a circular gold flag with a geometric surface area of 0.39 cm^2. A precursor solution consisting of 25 mM $LiNO_3$ + 50 mM $(Ni + Mn)(NO_3)_2$ ethanol solution, was pumped through the metal capillary nozzle at a rate of 2 ml h^{-1}. The Li : Ni : Mn molar ratio was adjusted to 1 : x : (2 − x). As a result of electrostatic forces, the precursor solution is atomized at the orifice of the nozzle and, consequently, a spray is generated and deposited as a thin layer (thickness: 0.5 μm) on the substrate. The substrate was placed 2.5 cm below the orifice of the capillary nozzle on a hotplate heated to 450 °C. After the deposition was finished, the substrate with the film was left on the heated hotplate to anneal for 1 h. Further annealing at 700 °C in air was carried out for 1 h. The film thickness was directly measured with a Dektak3 profilometer. The actual amount of $LiNi_xMn_{2-x}O_4$ (90 ± 5 μg) was estimated by weighing the electrode substrate before and after the film deposition using a Mettler Toledo MT5 microbalance.

XRD and Raman scattering measurements

A Shimadzu XD-D1 (Cu-Kα) instrument with an incident angle of 2° was used to obtain X-ray diffraction patterns to characterize the samples. The lattice parameter calculation was carried out with the LCR2 program.[26]

For the Raman measurements, the radiation employed was from either an argon ion laser (Coherent, Innova 70) operating at 514.5 and 457.9 nm, and 40 mW, or a krypton ion laser (Coherent, Innova 90 plus) operating at 647.1 nm and 40 mW focused on a spot (*ca.* 0.1 × 1.0 mm) of the working electrode surface with an incident angle of *ca.* 60°. Scattered light was

 DOI: 10.1039/b206764a

dispersed with a single grating spectrograph (Jasco, TRS-300) after pre-reduction of Rayleigh light with Raman-Super-Notch filters (Kaiser Optical Systems, Holographic Super Notch Plus -488, -514, and -647) and collected by an intensified diode array detector (Hamamatsu Photonics, M2492, M2493, and C2491). The spectra were obtained with a resolution of less than 2 cm^{-1}. It took about 10 min to collect each Raman spectrum.

In situ Raman during electrochemical measurements

For the simultaneous use of *in situ* Raman and cyclic voltammetry measurements, an airtight cell equipped with a random orientation quartz window (0.5 mm thick) was used.[27] Two lithium foils pressed on nickel meshes were used as the counter and the reference electrodes. The electrolyte was 1 M $LiBF_4$ in an ethylene carbonate (EC)–dimethyl carbonate (DMC) 1 : 1 by volume mixture. All the chemicals were Li ion battery grade and were purchased from Kishida Chemical. All potentials reported in this work are *versus* the Li/Li^+ reference electrode. The electrochemical cell was assembled in an argon-filled dry box (Miwa, MDB-1B + MS-P15S).

Raman spectra were collected after 2 successive potential scans between 3.4–5.0 V at 1 mV s^{-1}. Prior to each Raman measurement, the electrode potential was changed to the desired value and held there for at least 30 min (current was stable and less than 1 μA). The Li ion concentration in the $LiNi_xMn_{2-x}O_4$ film was considered to be at an equilibrium state during Raman measurements.

The electrode potential was controlled with a potentiostat (Hokuto Denko, HAB-151), and all measurements were carried out at room temperature (22 ± 2 °C).

Results

XRD characterization of $LiNi_xMn_{2-x}O_4$ thin films

The X-ray diffraction patterns of $LiNi_xMn_{2-x}O_4$ thin films prepared by ESD are shown in Fig. 1. All the peaks appearing in the XRD patterns for $LiNi_xMn_{2-x}O_4$ are very sharp, indicating that the samples have a high degree of crystallinity. The Miller index for each peak was determined based on a spinel structure of space group *Fd3m* and are indicated in Fig. 1. The lattice parameters were a = 8.225 Å for $LiMn_2O_4$, a = 8.212 Å for $LiNi_{0.2}Mn_{1.8}O_4$, and a = 8.172 Å for $LiNi_{0.5}Mn_{1.5}O_4$. This decrease in the lattice constant with increasing amounts of nickel is due to the increase in the concentration of Mn^{4+} ions in the spinel structure as Mn^{3+} ions are substituted with nickel ions.[15]

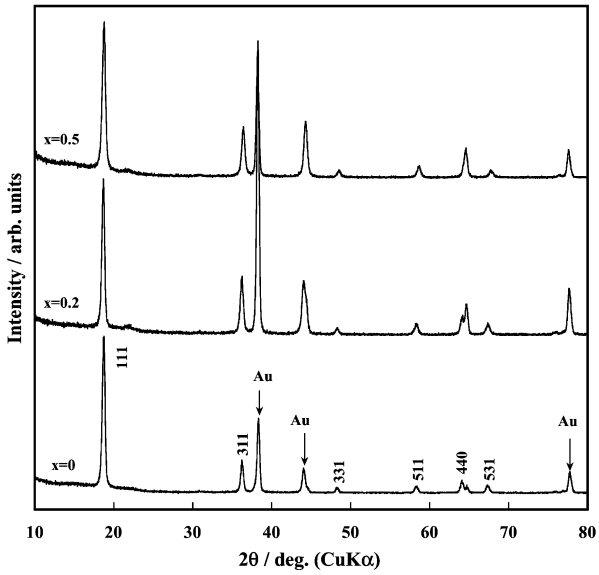

Fig. 1 XRD patterns of $LiNi_xMn_{2-x}O_4$ thin films deposited by ESD onto gold substrates.

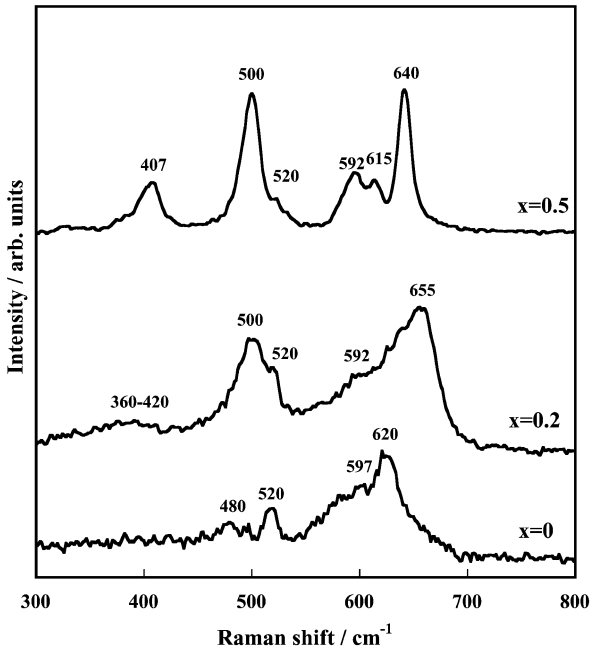

Fig. 2 *Ex situ* Raman spectra of the as-prepared $LiNi_xMn_{2-x}O_4$ pristine thin films recorded with 514.5 nm laser excitation.

Ex situ Raman characterization of thin films $LiNi_xMn_{2-x}O_4$

Fig. 2 shows conventional (*ex situ*) Raman spectra of fresh $LiNi_xMn_{2-x}O_4$ thin film electrodes. The Raman spectrum of the $LiMn_2O_4$ electrode consists of a series of broad bands between 450 and 700 cm^{-1}. The peaks at 620 (symmetric Mn–O stretching vibration of MnO_6 groups), 597, and 480 cm^{-1} are assigned to A_{1g}, $T_{2g}(3)$, $T_{2g}(2)$ modes, respectively, as predicted by group theory for a cubic compound.[28,29] Two other Raman-active modes predicted by calculations, one of E_g symmetry and the other $T_{2g}(1)$ symmetry, at 430 and 350 cm^{-1}, are not clearly visible in the spectrum of our $LiMn_2O_4$ thin film electrodes. In general, the Raman spectra of $LiMn_2O_4$ films prepared in our laboratory are nearly identical to those of bulk phase commercial $LiMn_2O_4$ powders (Nikki Chemicals, Japan), and $LiMn_2O_4$ thin films prepared by spin coating onto a Pt substrate[30] and pulsed layer deposition onto a stainless steel substrate[31] or onto silicon wafers.[32] Analysis of the 520 cm^{-1} band is problematic because the gold substrate also gives rise to a peak at the same wavelength.

Increasing the Ni content made the Raman spectra change in a complicated manner. The following observations can be made. (i) The 620 cm^{-1} band that is associated with the symmetric Mn–O stretching vibration of the MnO_6 groups shifted slightly to 615 cm^{-1}. (ii) New features at 407 and 500 cm^{-1} became sharper and grew in intensity with increasing nickel content, and thus can be unequivocally be attributed to the Ni^{2+}–O stretching mode in the structure.[33] (iii) A broad band at 655 cm^{-1} appeared for the $LiNi_{0.2}Mn_{1.8}O_4$ film, which shifted to 640 cm^{-1} for $LiNi_{0.5}Mn_{1.5}O_4$. These bands are typically observed for haussmanite Mn_3O_4 and bixbyite Mn_2O_3.[28,29]

Characterization using cyclic voltammetry

Fig. 3 shows cyclic voltammograms (CV) of $LiNi_xMn_{2-x}O_4$ thin film electrodes at a scan rate of 0.1 mV s^{-1} in $LiBF_4$–EC–DMC solution. As can be seen in Fig. 3, the nickel-containing sample gives an operating voltage greater than 4.5 V, in

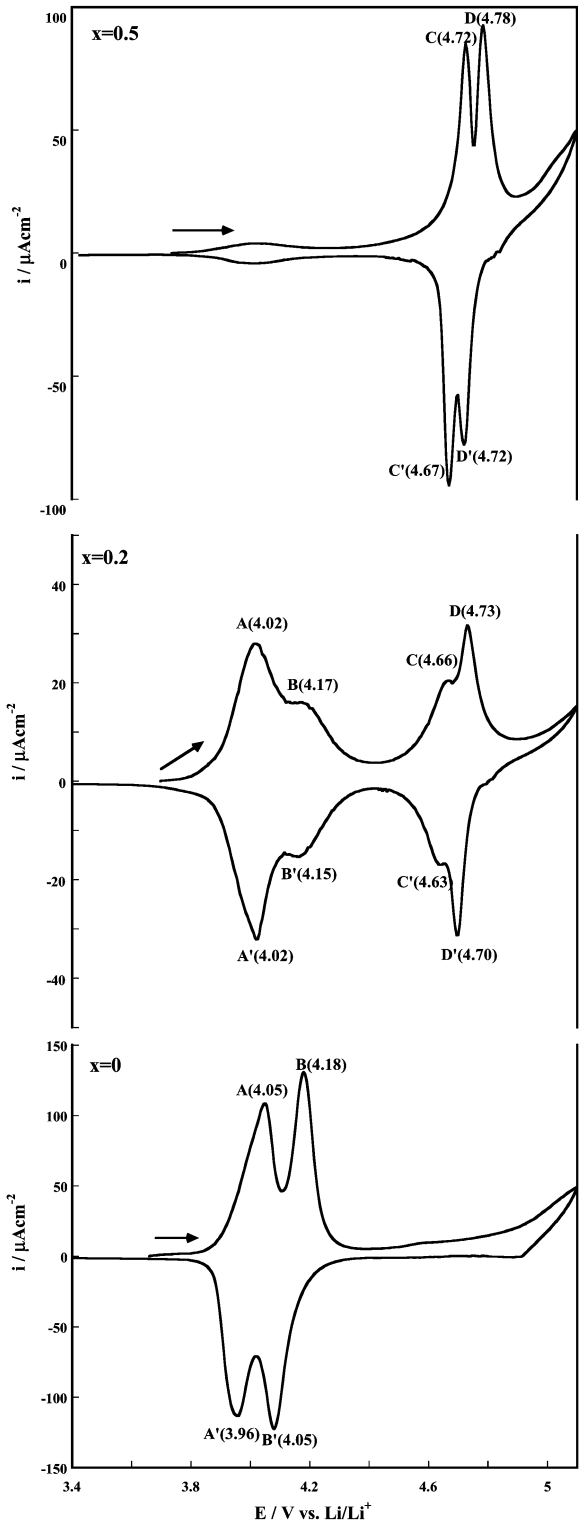

Fig. 3 Cyclic voltammograms of $LiNi_xMn_{2-x}O_4$ thin films taken at a scan rate of 0.1 mV s^{-1} in 1 M $LiBF_4$–EC–DMC solution.

comparison to the normal operating voltage around 4.0 V observed for $LiMn_2O_4$. From Fig. 3, it is also clear that the current related to the 4.7 V signal increases with increasing the nickel content in the spinel. The current increase above 4.7 V is due to the oxidation of electrolyte.

The oxidation state of manganese in $LiMn_2O_4$ is 3.5, and it can be described as $LiMn^{3+}Mn^{4+}O_4$. Li ion extraction and insertion take place with the redox of $Mn^{3+/4+}$ in the structure at 4 V; Mn^{3+} is totally absent when Li ions are completely extracted from the structure. In the case of $LiNi_xMn_{2-x}O_4$, substitution metal ions (Ni^{2+}) exist at the 16d site, instead of Mn^{3+}, and their redox reactions are related to the Li ion extraction/insertion at 5 V.[19]

The changes in CV depending on Ni content can be explained as follows. Assuming that all the Ni ions present in the spinel phase are divalent, the oxidation states of the manganese in the spinel can be expressed as $Li^{+}Ni^{2+}{}_{x}Mn^{3+}{}_{1-2x}Mn^{4+}{}_{1+x}O^{-2}{}_{4}$.[10] The current response at 4.7 V would then correspond to the redox of $Ni^{2+/4+}$ in the structure.[15] Thus, at $x = 0.5$, there will be no Mn^{3+} in the spinel and the redox couple $Mn^{3+/4+}$ at 4 V is barely seen for the spinel $LiNi_{0.5}Mn_{1.5}O_4$.

In situ Raman measurements

In situ Raman spectra recorded at various potentials for $LiNi_xMn_{2-x}O_4$ thin films in $LiBF_4$–EC–DMC solution were first collected with 514.5 nm excitation and are shown in Fig. 4. The electrode was initially charged to 5.00 V and then the electrode potential was reduced to 3.40 V. The strong band at *ca.* 592 cm^{-1} for $LiMn_2O_4$ is similar to that observed for λ-MnO_2 by Kanoh *et al.*[28] for the fully delithiated spinel manganese oxide. The vibration modes of $LiMn_2O_4$ and λ-MnO_2 are described in detail in ref. 29.

In situ Raman spectra of $LiNi_{0.2}Mn_{1.8}O_4$ and $LiNi_{0.5}Mn_{1.5}O_4$ show only weak broad bands within the 3.4–4 V range. When the potential was increased from 4.05 to 5 V, the following observations were made.

A new band at *ca.* 540 cm^{-1} for both $LiNi_{0.2}Mn_{1.8}O_4$ and

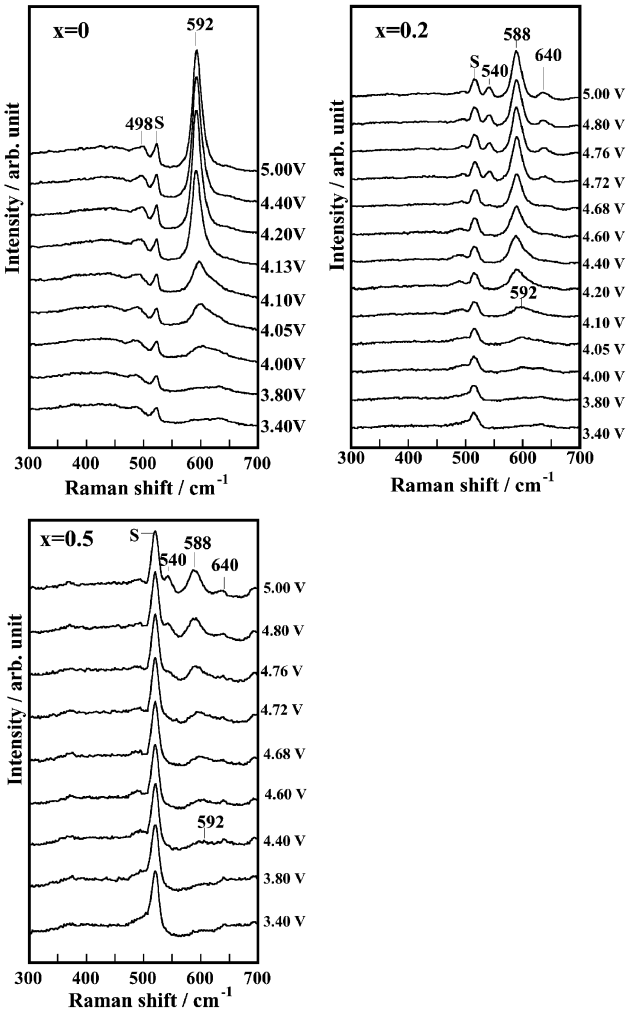

Fig. 4 *In situ* Raman spectra of $LiNi_xMn_{2-x}O_4$ thin film electrodes recorded with 514.5 nm radiation. The electrode potential was changed from 5.00 to 3.40 V.

$LiNi_{0.5}Mn_{1.5}O_4$ appeared for potentials greater than 4.72 V, corresponding to the CV peak D/D′ in Fig. 3. The Raman peak at 540 cm^{-1} can be viewed as due to the symmetric O–Ni–O stretching vibration. Desilvestro *et al.*[34] suggested that this Raman band is due to the Ni^{4+}–O bond.

A 588 cm^{-1} band appeared, starting at 4.2 V. The intensity of the 588 cm^{-1} band is obviously reduced as the Ni content increases in the spinel structure, which might be caused by the decreasing amount of Mn^{4+} at the film surface as the amount of Ni increases. The Li ion extraction/insertion at 4.7 V is due to the redox of $Ni^{2+/4+}$, and the oxidation state of Mn, at +4, should be constant above 4.4 V. These results suggest that the 588 cm^{-1} band depends on not only the oxidation state of Mn, but also on the Li ion concentration at the 8a sites. The band at *ca.* 520 cm^{-1} is independent of the potential and, thus, is ascribed to the gold substrate and/or to the $LiBF_4$–EC–DMC solution, which also gives rise to a band at the same wavelength (Fig. 5). When the materials were discharged from 3.4 to 5.0 V, the observed spectral changes were the reverse of those observed during the initial charge process and the spectra are omitted here.

Effect of the laser excitation

To gain further insight into the electronic structure dependence on the vibrational features of $LiNi_{0.5}Mn_{1.5}O_4$, we have studied its Raman spectrum as a function of the laser line energy. Fig. 6 shows the effect of the laser line excitation for λ = 457.9, 514.5, and 647.1 nm at a potential of 5.00 V. Raman peaks appeared at the same frequency, but changes in peak intensities were observed, *e.g.* strong enhancement of the 540 cm^{-1} band. The increase in $I(540)/I(588)$ provides direct evidence of electronic resonance in $LiNi_{0.5}Mn_{1.5}O_4$. This indicates that resonance enhancement exists for $Ni_{0.5}Mn_{1.5}O_4$, which seems analogous to the case of λ-MnO_2.[29]

The band at *ca.* 685 cm^{-1} is due to the solution (shoulder in Fig. 5). The small peak at 670 cm^{-1} was seen only with 647.1 nm excitation and was not observed in Raman spectra of the solution with the same laser excitation. Its cause is unknown, but it may be due to the formation of an interfacial layer between the substrate and the film.

Subsequently, *in situ* Raman spectra of $LiNi_{0.5}Mn_{1.5}O_4$ were collected again with a laser wavelength of 647.1 nm at various potentials, and results are shown in Fig. 7. It can be seen that the changes in the Raman spectra are reversible upon changing the electrode potential, which suggests that the reversibility of the Li ion extraction and insertion is good. At 3.40 V, the

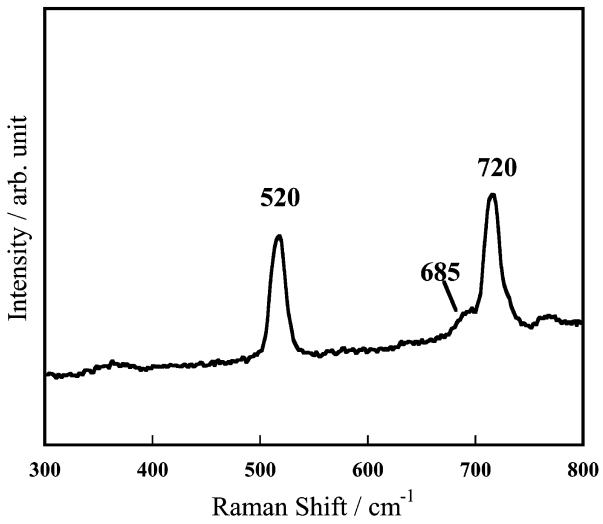

Fig. 5 *Ex situ* Raman spectra of $LiBF_4$–EC–DMC solution recorded with 514.5 nm radiation.

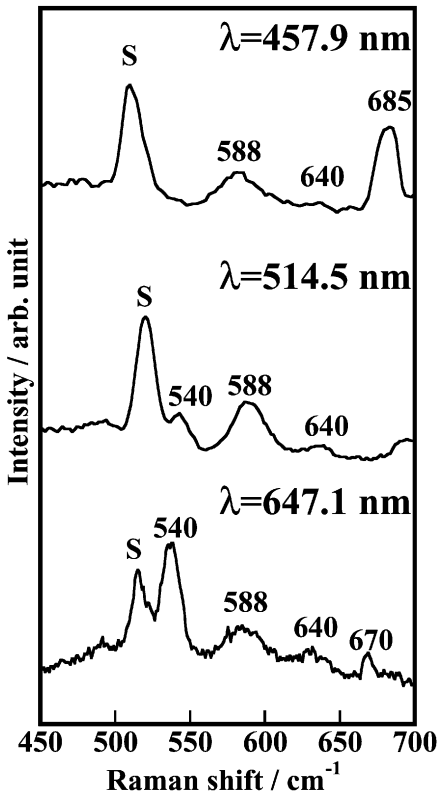

Fig. 6 *In situ* Raman spectra of a $LiNi_{0.5}Mn_{1.5}O_4$ thin film electrode at a potential of 5.00 V, recorded with various laser excitation wavelengths (indicated on the figure).

characteristic Ni^{2+}–O vibration at *ca.* 500 cm^{-1} (observed in the *ex situ* Raman shown in Fig. 2) can be clearly seen with 647.1 nm excitation. It is interesting to note that the 500 cm^{-1} band shifted to 488 cm^{-1} as the potential increased from 3.40 to 4.68 V. According to Delichere *et al.*[35] and Cordoba-Torresi *et al.*,[33b] the 488 cm^{-1} band is due to the Ni^{3+}–O stretching mode. Therefore, the peak shift from 500 to 488 cm^{-1} indicates that the Ni is oxidized from Ni^{2+} to Ni^{3+}, which is in agreement with the XAFS results reported by Terada *et al.*[24] Indeed, the capacities of CV peaks C and D were calculated, by integration of the current in Fig. 3(c), to be 68.0 and 69.5 $mAhg^{-1}$, respectively. This means that the average oxidation state of Ni should be 3 at the midpoint of the peak C and D. Above 4.72 V, the 488 cm^{-1} band is no longer seen, whereas a peak at 540 cm^{-1} appears, the intensity of which increases up to 5.00 V. This suggests that the Ni is further oxidized from Ni^{3+} to Ni^{4+}. Based on the results of *in situ* Raman spectra of $LiNi_xMn_{2-x}O_4$ thin films, the Li ion extraction and insertion at 4.7 V can be properly explained as follows. During CV peak C/C′ in Fig. 3, the Li ion extraction and insertion proceeds due to the redox of $Ni^{2+/3+}$, and at CV peak D/D′, due to the redox of $Ni^{3+/4+}$, while both CV peaks A/A′ and B/B′ correspond to the redox of $Mn^{3+/4+}$ in the spinel structure.

Conclusions

The present work is to first to address *in situ* Raman spectroscopic studies of $LiNi_xMn_{2-x}O_4$ ($0 \leqslant x \leqslant 0.5$) thin film cathodes prepared by the electrostatic spray deposition method. The overall picture that emerges from these studies is as follows.

Ex situ Raman spectra of $LiNi_xMn_{2-x}O_4$ revealed that the Ni^{2+}–O stretching mode in the structure has characteristic vibrations *ca.* 407 and 500 cm^{-1}. Bands around 655–640 cm^{-1},

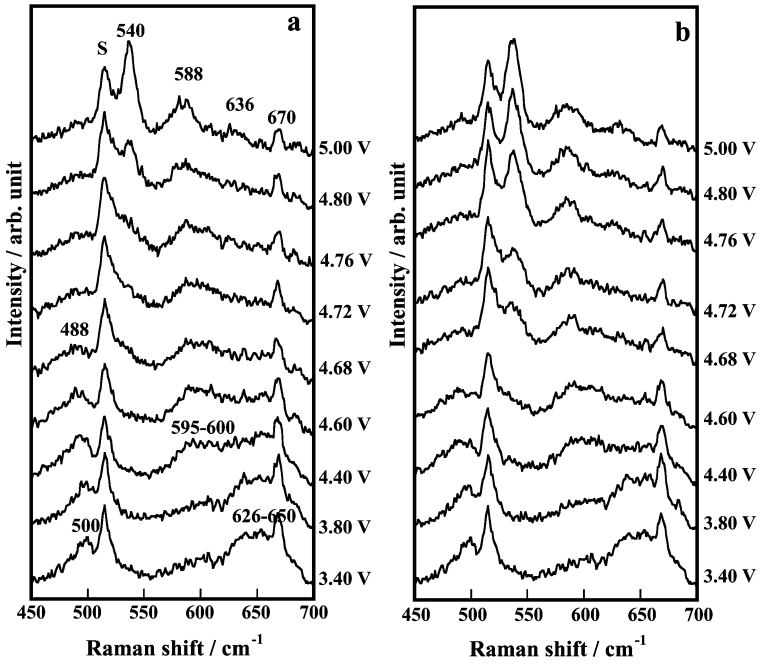

Fig. 7 *In situ* Raman spectra of a Li $Ni_{0.5}Mn_{1.5}O_4$ thin film electrode recorded with the 647.1 nm laser excitation: (a) the electrode potential was changed from 3.40 to 5.00 V, and (b) from 5.00 to 3.40 V.

characteristic of Mn_3O_4 and Mn_2O_3, were recoded for $LiNi_xMn_{2-x}O_4$ ($x > 0$).

From the *in situ* Raman spectral changes observed for the thin films in an organic electrolyte during Li ion extraction and insertion in the potential range 3.4–5.0 V, it is suggested that Li ion extraction and insertion around 4.7 V proceeds as follows. The redox of $Ni^{2+/3+}$ takes place in the potential range 4.4–4.7 V and of $Ni^{3+/4+}$ at 4.7–5.0 V in the spinel structure, while the redox in 3.8–4.4 V corresponds to $Mn^{3+/4+}$. In addition, it was confirmed that these changes in the Raman spectra were reversible upon changing the electrode potential, and that the Li ion extraction and insertion proceeded in reversible manner.

Acknowledgements

K. D. acknowledges a research fellowship from the Japan Society for the Promotion of Science. M. M is indebted to the Ministry of Education, Culture, Sports, Science, and Technology, Japan, for a Grant-in-Aid for the Encouragement of Young Scientists (No. 13750755).

References

1 M. M. Thackeray, *Prog. Solid State Chem.*, 1997, **25**, 1–71.
2 J. M. Tarascon and D. Guyomard, *Electrochim. Acta*, 1993, **38**, 1221–1231.
3 T. Ohzuku, M. Kitagawa and T. Hirai, *J. Electrochem. Soc.*, 1990, **137**, 769–774.
4 Y. Xia and M. Yoshio, *J. Electrochem. Soc.*, 1996, **143**, 825–833.
5 J. M. Tarascon, E. Wang, F. K. Shokoohi, W. R. McKinnon and S. Colson, *J. Electrochem. Soc.*, 1991, **138**, 2859–2863.
6 J. M. Tarascon, W. R. McKinnon, F. Coowar, T. N. Bowmer, G. Amatucci and D. Guyomard, *J. Electrochem. Soc.*, 1994, **141**, 1421–1431.
7 R. J. Gummow, A. De Kock and M. M. Thackeray, *Solid State Ionics*, 1994, **69**, 59–63.
8 Y. Gao and J. R. Dahn, *J. Electrochem. Soc.*, 1996, **143**, 1783–1788.
9 L. Guohua, H. Ikuta, T. Uchida and M. Wakihara, *J. Electrochem. Soc.*, 1996, **143**, 178–182.
10 K. Amine, H. Tukamoto, H. Yasuda and Y. Fujita, *J. Electrochem. Soc.*, 1996, **143**, 1607–1612.
11 W. Liu, K. Kowal and G. C. Farrington, *J. Electrochem. Soc.*, 1996, **143**, 3590–3596.
12 Y. Xia and M. Yoshio, *J. Electrochem. Soc.*, 1997, **144**, 4186–4194.
13 S. T. Myung, S. Komaba and N. Kumagai, *J. Electrochem. Soc.*, 2001, **148**, A482–A489.
14 (*a*) C. Sigala, D. Guyomard, A. Verbaere, Y. Piffard and M. Tournoux, *Solid State Ionics*, 1995, **81**, 167–170; (*b*) C. Sigala, A. Verbaere, J. L. Mansot, D. Guyomard, Y. Piffard and M. Tournoux, *J. Solid State Chem.*, 1997, **132**, 372–381.
15 Q. Zhong, A. Bonakdarpour, M. Zhang, Y. Gao and J. R. Dahn, *J. Electrochem. Soc.*, 1997, **144**, 205–213.
16 H. Kawai, M. Nagata, H. Kageyaama, H. Tukamoto and A. R. West, *Electrochim. Acta*, 1999, **45**, 315–327.
17 (*a*) H. Kawai, M. Nagata, M. Tabuchi, H. Tukamoto and A. R. West, *Chem. Mater.*, 1998, **10**, 3266–3268; (*b*) H. Shigemura, H. Sakaebe, H. Kageyama, H. Kobayashi, A. R. West, R. Kanno, S. Morimoto, S. Nasu and M. Tabuchi, *J. Electrochem. Soc.*, 2001, **148**, A730–A736.
18 (*a*) Y. Ein-Eli and W. F. Howard, *J. Electrochem. Soc.*, 1997, **144**, L205–L207; (*b*) Y. Ein-Eli, J. T. Vaughey, M. M. Thackeray, S. Mukerjee, X. Q. Yang and J. McBreen, *J. Electrochem. Soc.*, 1999, **146**, 908–913.
19 T. Ohzuku, S. Takeda and M. Iwanaga, *J. Power Sources*, 1999, **81-82**, 90–94.
20 K. Amine, H. Tukamoto, H. Yasuda and Y. Fujita, *J. Power Sources*, 1997, **68**, 604–608.
21 K. Dokko, M. Nishizawa and I. Uchida, *Denki Kagaku oyubi Kogyo Butsuri Kagaku*, 1998, **66**, 1188–1193.
22 K. Kanamura, W. Hoshikawa and T. Umegaki, *J. Electrochem. Soc.*, 2002, **149**, A339–A345.
23 R. Alcántara, M. Jaraba, P. Lavela and J. L. Tirado, *Electrochim. Acta*, 2002, **47**, 1829–1835.
24 Y. Terada, K. Yasaka, F. Nishikawa, T. Konishi, M. Yoshio and I. Nakai, *J. Solid State Chem.*, 2001, **156**, 286–291.
25 (*a*) M. Nishizawa, T. Uchiyama, T. Itoh, T. Abe and I. Uchida, *Langmuir*, 1999, **15**, 4949–4951; (*b*) T. Uchiyama, M. Nishizawa, T. Itoh and I. Uchida, *J. Electrochem. Soc.*, 2000, **147**, 2057–2060.
26 D. E. Williams, Ames Laboratory Report IS-1052, Ames Laboratory, Ames, IA, USA, 1964.
27 T. Itoh, K. Abe, M. Mohamedi, M. Nishizawa and I. Uchida, *J. Solid State Electrochem.*, 2001, **5**, 328–333.
28 H. Kanoh, W. Tang and K. Ooi, *Electrochem. Solid-State Lett.*, 1998, **1**, 17.
29 B. Ammundsen, G. R. Burns, M. S. Islam, H. Kanoh and J. Roziere, *J. Phys. Chem. B*, 1999, **103**, 5175–5180.
30 W. Huang and R. Frech, *J. Power Sources*, 1999, **81-82**, 616–620.
31 Y. Luo, W. B. Cai and D. A. Scherson, *Electrochem. Solid-State Lett.*, 2001, **4**, A101–A104.
32 Y. Matsuo, R. Kostecki and F. McLarnon, *J. Electrochem. Soc.*, 2001, **148**, A687–A692.

33 (*a*) P. Delichere, S. Joiret, A. Hugot-le Goff, K. Bange and B. Hetz, *J. Electrochem. Soc.*, 1998, **135**, 1856–1857; (*b*) S. I. Cordoba-Torresi, A. Hugot-le Goff and S. Joiret, *J. Electrochem. Soc.*, 1991, **138**, 1554–1558.
34 (*a*) J. Desilvestro, D. Corrigan and M. J. Weaver, *J. Phys. Chem.*, 1986, **90**, 6408–6411; (*b*) J. Desilvestro, D. Corrigan and M. J. Weaver, *J. Electrochem. Soc.*, 1988, **135**, 885–891.
35 P. Delichere, A. Hugot-le Goff and N. Yu, *J. Electrochem. Soc.*, 1986, **133**, 2106–2107.